Journal of Cerebral Blood Flow & Metabolism (2013) 33, 935–943

www.jcbfm.com

ORIGINAL ARTICLE

Irradiation to the young mouse brain caused long-term, progressive depletion of neurogenesis but did not disrupt the neurovascular niche

Martina Boström[1], Marie Kalm[1], Niklas Karlsson[2], Nina Hellström Erkenstam[1] and Klas Blomgren[1,2,3]

We investigated the effects of ionizing radiation on microvessel structure and complexity in the hippocampus. We also assessed neurogenesis and the neurovascular niche. Postnatal day 14 male C57BL/6 mice received a single dose of 8 Gy to the whole brain and were killed 6 hours, 1 week, 7 weeks, or 1 year later. Irradiation decreased the total number of microvessels and branching points from 1 week onwards and decreased the total microvessel area 1 and 7 weeks after irradiation. After an initial increase in vascular parameter densities, concomitant with reduced growth of the hippocampus, the densities normalized with time, presumably adapting to the needs of the surrounding nonvascular tissue. Irradiation decreased the number of neural stem and progenitor cells in the hippocampus. The relative loss increased with time, resulting in almost completely ablated neurogenesis (DCX^+ cells) 1 year after irradiation (77% decreased 1 week, 86% decreased 7 weeks, and 98% decreased 1 year after irradiation compared with controls). After irradiation, the distance between undifferentiated stem cells and microvessels was unaffected, and very few dying endothelial cells were detected. Taken together, these results indicate that the vasculature adjusts to the surrounding neural and glial tissue after irradiation, not vice-versa.

Journal of Cerebral Blood Flow & Metabolism (2013) **33,** 935–943; doi:10.1038/jcbfm.2013.34; published online 13 March 2013

Keywords: angiogenesis; endothelium; hippocampus; neural stem cells; radiotherapy

INTRODUCTION

Brain tumors account for 20–30% of all childhood cancers, making them the second most common type of pediatric cancers after leukemias.[1,2] The Nordic countries have among the highest incidence rates in the world[3] and radiotherapy is commonly used in the treatment of these tumors. However, there are several long-term debilitating effects following radiotherapy in children, including cognitive decline and motor, hormonal and psychological–emotional dysfunctions.[4,5] Furthermore, survivors of childhood cancer have an increased risk of long-term cerebrovascular mortality, and the risk of death from cerebrovascular disease increases linearly with the local radiation dose to the prepontine cistern.[6]

More than four centuries ago, it was observed that the vascular and the nervous systems show similar anatomical patterning. Vascular outgrowth has been observed to precede neural axon outgrowth in the developing mouse embryo. This robust generation of a vascular plexus in the embryo is later followed by remodeling into fine capillary networks.[7] Paradoxically, it has been suggested that peripheral nerves in turn provide a template for this vascular remodeling and determines the patterning of arterial differentiation and blood vessel branch patterning in the skin. In addition, arteries are specifically aligned with peripheral nerves.[8] It therefore appears as if the vasculature and the nervous system during development and beyond are interdependently regulated and a change in one can alter the other.

Decades ago, it was hypothesized that the damage observed in the brain following irradiation was mainly due to microvessel damage that in turn caused ischemia and necrosis. This hypothesis was supported by alterations to capillaries that preceded general tissue necrosis, such as thickening of the capillary basal lamina.[9] In addition, cranial irradiation has previously been demonstrated to cause widely scattered minute necrotic lesions in the forebrain white matter of adult monkeys subjected to 60 Gy fractionated irradiation. The number of lesions increased with time after treatment and were accompanied by both focal vascular endothelial hyperplasia as well as patches of telangiectasias.[10] The prevailing view was that the radiosensitivity of the brain and spinal cord was mediated in large part by the response of cerebrovascular wall elements and that these responses constituted the primary limitation of radiotherapy.[11] Today, much attention is instead focused on the birth of new neurons in the postnatal brain.[12] As a result, it was revealed that areas in the brain where postnatal neurogenesis occurs are particularly

[1]Center for Brain Repair and Rehabilitation, Institute of Neuroscience and Physiology, Sahlgrenska Academy, University of Gothenburg, Gothenburg, Sweden; [2]Department of Women's and Children's Health, Karolinska Institutet, Karolinska University Hospital, Stockholm, Sweden and [3]Department of Pediatrics, University of Gothenburg, Queen Silvia Children's Hospital, Gothenburg, Sweden. Correspondence: Professor K Blomgren, Department of Women's and Children's Health, Karolinska Institutet, Karolinska University Hospital, Q2:07, Stockholm SE 171 76, Sweden.
E-mail: klas.blomgren@ki.se
This work was supported by the Swedish Childhood Cancer Foundation (Barncancerfonden), the Swedish Research Council (Vetenskapsrådet), governmental grants from *Agreement concerning research and education of doctors* (ALF), the Sahlgrenska Academy at the University of Gothenburg, the Sten A Olsson's Foundation, the King Gustav V Jubilee Clinic Research Foundation (JK-fonden), the Frimurare Barnhus Foundation, the Wilhelm and Martina Lundgren Foundation, the Gothenburg Medical Society, Sahlgrenska Foundations (SU-fonden), the Aina Wallström's and Mary-Ann Sjöblom's Foundation, the Ulla and Rune Amlöv Foundations, AFA Insurance, and the Swedish Society of Medicine.
Received 26 September 2012; revised 21 January 2013; accepted 12 February 2013; published online 13 March 2013

sensitive to radiotherapy and that loss of these stem/progenitor cells may contribute to the cognitive deficits observed after radiation therapy.[12,13] A critical, but poorly understood regulator of neurogenesis is the role that blood vessels play in nurturing newborn cells. Proliferating cells in the hippocampus are vascular-associated, that is, they are born in close proximity to blood vessels and blood vessels appear to be critical in providing support for these cells.[14,15] In addition, endothelial cells are believed to have direct cell-to-cell contact with stem cells to increase neuronal survival.[16] It is therefore important to consider the effect on the vasculature when investigating radiation-induced outcomes in neurogenesis.

Most studies have focused on how adult and mature brain tissue responds to radiation therapy. Considerably fewer studies have investigated the effects of irradiation on the young, developing brain and very little is known about how microvessels in the hippocampus respond to this type of insult.[17–19] Therefore, the primary aim of this study was to investigate how microvessels in the hippocampus were affected by irradiation to the young mouse brain, by quantifying blood vessel parameters at different time points after irradiation. We also sought to investigate the role of the neurovascular niche in the support and survival of neural stem/progenitor cells.

MATERIALS AND METHODS

Animals

Male C57BL/6 mice were delivered on postnatal day 9 (P9) from Charles River Breeding Laboratories (Sulzfeld, Germany). The animals were housed with a reversed 12-hour dark–light cycle (light between 2100 and 0900 hours) at constant temperature (24°C) and relative humidity (50–60%), with *ad libitium* access to food and water. After weaning, all animals were kept in cages with three animals per cage. All experiments were approved by the Swedish Animal Welfare Agency (Gothenburg animal ethics application no. 423/2008 and no. 326/2009).

Irradiation Procedure

A linear accelerator (Varian Clinac 600 CD, Radiation Oncology Systems LLC, San Diego, CA, USA) with 4 MV nominal photon energy and a dose rate of 2.3 Gy/min was used to irradiate mice on P14. The mice were anesthetized with an intraperitoneal injection of tribromoethanol (50 mg/kg; Sigma, Stockholm, Sweden), placed on a polystyrene bed in a prone position (head to gantry) and irradiated with a symmetrical 2×2 cm radiation field. The head was covered with a 1-cm tissue equivalent material to obtain an even radiation dose in the recipient tissue. Source to skin distance was ~ 99.5 cm and the irradiated tissue received a single absorbed dose of 8 Gy with a dose variation of $\pm 5\%$. The animals were kept on a warm bed (36°C) both before and after irradiation to maintain body temperature. Control animals were anesthetized but did not receive any irradiation.

Tissue Preparation

Animals (six controls and six irradiated for each time point) were deeply anesthetized with sodium pentobarbital (Pentothal; Electra-box Pharma, Tyresö, Sweden) and transcardially perfused with 0.9% saline, followed by 4% paraformaldehyde, 6 hours, 1 week (8 days), 7 weeks, or 62 weeks (in the text referred to as the '1-year' group) after irradiation. The brains were removed and postfixed for 24 hours in paraformaldehyde at 4°C before being transferred to a 30% sucrose solution (30% sucrose in 0.1 M phosphate buffer).

After equilibration in sucrose, the brains were fixed with a cryo-gel (Tissue-Tec O.C.T compound) to a dry ice-cooled copper block and one hemisphere was sagitally cut into 25-μm sections with a sliding microtome (Leica SM2000R, Leica Microsystems, Nussloch, Germany). Serial sections were collected in a series of 10 (1-week group) or 12 (6 hours, 7 weeks, and 1-year groups) tubes containing TCS (tissue cryoprotectant solution; 25% ethylene glycol, 25% glycerin, and 0.05 M phosphate buffer), and stored at 4°C until used for immunohistochemistry.

Immunohistochemistry

Stainings for Stereological Quantifications. Stainings for stereological analysis were performed on every 10th (1-week group) or 12th (7 weeks and 1-year groups) section and rinsed in Tris-buffered saline (TBS; 0.08 mol/L Trizma-HCl, 0.016 mol/L Trizma-Base, 0.15 mol/L NaCl, pH 7.5) before staining. Antigen retrieval was performed on sections for doublecortin (DCX) staining, consisting of 30 minutes incubation in 80°C sodium citrate (10 mM, pH 9.0). Sections for cluster of differentiation 31 (CD31, also called platelet endothelial cell adhesion molecule-1 [PECAM-1]) staining did not undergo any pretreatment. After rinsing in TBS, the sections underwent two subsequent steps to avoid unspecific binding. First, endogenous peroxidase activity was blocked by incubating the sections in 30% hydrogen peroxide (H_2O_2) for 30 minutes, followed by rinsing in TBS. This was followed by 30 minutes incubation in TBS with 3% donkey serum and 0.1% Triton X-100 (blocking solution) to avoid unspecific antigen binding. Sections were incubated with primary antibodies diluted in blocking solution at 4°C for either 24 hours (monoclonal rat anti-mouse CD31, 1:2,000, BD Bioscience Pharmigen, Franklin Lakes, NJ, USA) or 72 hours (polyclonal goat anti-DCX, 1:125, Santa Cruz Biotechnology, Santa Cruz, CA, USA). After rinsing in TBS, sections were incubated at room temperature for 1 hour with biotinylated secondary antibodies diluted 1:1,000 in blocking solution; donkey anti-rat IgG or donkey anti-goat IgG (Jackson ImmunoResearch Laboratories, West Grove, PA, USA). This was followed by rinsing and amplification with avidin–biotin enzyme complex (ABC kit, Vectastain Elite, Vector Laboratories, Burlingame, CA, USA) for 1 hour, and finally incubation in detection solution (0.25 mg/mL diaminobenzidine, 0.009% H_2O_2, 0.04% $NiCl_2$) for visualization.

Immunofluorescence. For double and triple stainings, every 12th section was used to quantify numbers of dying endothelial cells (CD31, active caspase-3, and TO-PRO) and the distance between stem cells and nearest microvessel (CD31 and brain lipid-binding protein (BLBP)). Sections were rinsed in TBS and incubated in blocking solution for 30 minutes, followed by rinsing and incubation for 72 hours at 4°C with primary antibodies: rat anti-mouse CD31 (1:500), rabbit anti-BLBP (1:500, Millipore, Temecula, CA, USA) and rabbit anti-active caspase-3 (1:250, BD Bioscience Pharmigen). Sections were then rinsed and incubated with appropriate fluorescent secondary antibodies for 2 hours: donkey anti-rat Alexa 488, donkey anti-rabbit Alexa 647, donkey anti-rabbit Alexa 555 (all 1:1,000, Invitrogen/Molecular Probes, Carlsbad, CA, USA), and TO-PRO-3 Iodide (1:4,000, Invitrogen/Molecular Probes).

Stereological Principles for Microvessel Analysis

To quantify and characterize microvessels in the brain, the following parameters were analyzed:

- area covered by microvessels
- number of microvessels
- diameter of the microvessels
- number of microvessel branching points

This was assessed in one neurogenic hippocampal area (i.e., the granule cell layer; GCL) and two adjacent nonneurogenic hippocampal areas (the hilus and the molecular layer; ML), using a Leica DM6000B microscope (Leica, Wetzlar, Germany) and the *area fraction fractionator* method in the stereology system Stereo Investigator (MBF Bioscience, Williston, VT, USA). The counting frames used were 75×25 μm for the GCL and hilus and 50×50 μm for the ML, and were randomly distributed by the software with a grid overlay of 210×75 μm, 210×65 μm, or 275×100 μm for the GCL, hilus, and ML, respectively. The size of the counting frame and grid overlay were established for each structure to achieve the best-calculated estimate. The area was traced at $\times 10$ magnification with a DIC filter, while counting and measurements were performed at $\times 40$ magnification.

The counting frame had an overlay of crosses every 5 μm to estimate the total area covered by blood vessels (10×10 crosses for ML (Figure 1A) and 5×15 crosses for GCL and hilus). Every cross that touched a vessel was marked and the total number of marked crosses was summed up. Each cross represented an area of 25 μm^2 (5×5 μm). The total area covered by vessels was calculated by first multiplying the total number of marked crosses with the corresponding area of each cross (25 μm^2). This was then divided with the fraction of the sampled area and the total traced areas, and finally multiplied by the series (10 or 12). The sampled area is the total number of analyzed counting frames multiplied with the counting frame area (1,875 μm^2 (75×25 μm) for the GCL and hilus and 2,500 μm^2 (50×50 μm) for the ML). The total number of vessels was quantified by counting the number of vessels that crossed any of the four borders of the

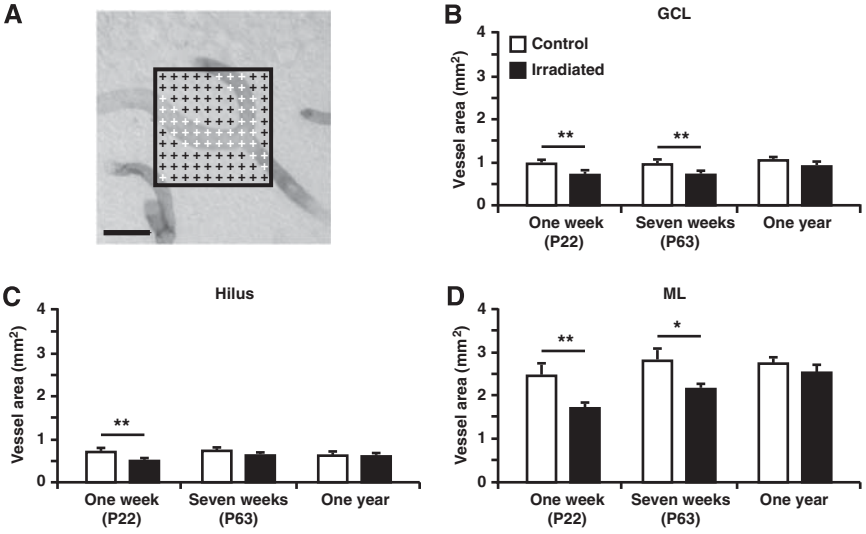

Figure 1. The total area covered by microvessels in the granule cell layer (GCL), hilus, and molecular layer (ML) of the dentate gyrus. (**A**) Representative picture displaying the overlay of crosses used to quantify the total vessel area, as described in the Materials and methods section. Crosses that touch a microvessel are white and those that do not are black. The total number of white crosses was used to obtain the total area covered by vessels. The graphs show quantifications in the GCL (**B**), hilus (**C**), and ML (**D**) 1 week, 7 weeks, and 1 year after irradiation. Postnatal day (P), $n = 6$ per group, group mean values ± s.e.m., scale bar = 20 μm, $^{*}P < 0.05$, $^{**}P < 0.01$.

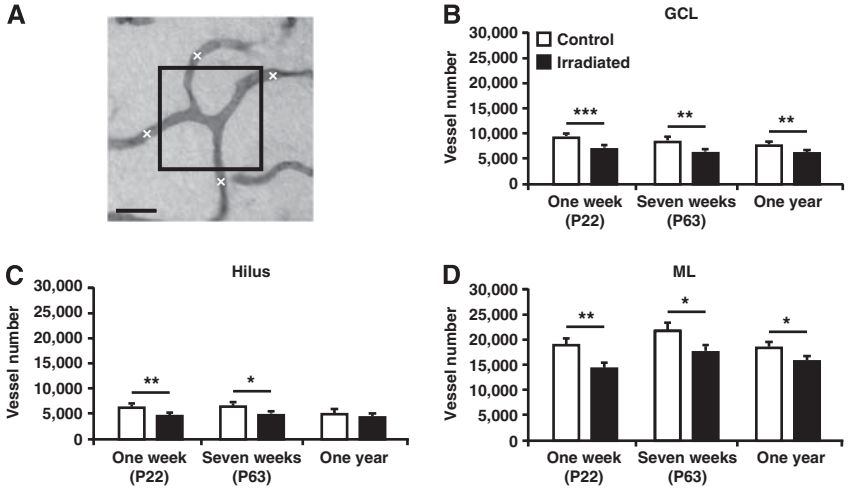

Figure 2. Quantification of the number of microvessels in the granule cell layer (GCL), hilus, and molecular layer (ML) of the dentate gyrus. (**A**) Schematic picture illustrating how the quantification of vessels was performed by using the *area fraction fractionator* method, as described in the Materials and methods section. The boxes were randomly placed within the structure and all vessels crossing any of the borders of the box were counted to obtain the total number of microvessels. The graphs show quantifications in the GCL (**B**), hilus (**C**), and ML (**D**) 1 week, 7 weeks, and 1 year after irradiation. Postnatal day (P), $n = 6$ per group, group mean values ± s.e.m., scale bar = 20 μm, $^{*}P < 0.05$, $^{**}P < 0.01$, $^{***}P < 0.001$.

counting frame (Figure 2A). This number was then multiplied by the fraction of the sampled and the traced areas, multiplied by the series. The diameter of all the counted vessels was measured using the *quick measurement tool* and an average diameter was calculated for each structure. Capillary diameter does not change in the postnatal brain, and since it was found to be highly consistent in the brains prepared on the same occasion, this diameter was used to normalize between brains prepared under slightly different conditions. Branching points were quantified without the area fraction fractionator; hence, all branching points were counted and multiplied by the series to obtain the total number. The investigator performing the counting was blinded to the treatment of the animals.

Quantification of Neuronal Precursor Cells

Stereo Investigator and the previously mentioned Leica microscope were used to trace the GCL at × 10 magnification and count the DCX-positive cells in the GCL plus two cell layers (one cell diameter defined as 6 μm) into the hilus at × 40 magnification. The number of counted cells was then multiplied with the series to obtain the total number of cells.

Cell Death Analysis

To evaluate whether irradiation induced endothelial cell death, sections from 6 hours after irradiation where scanned with a confocal Leica TCS SP2 microscope at × 20 magnification to visualize cells double-positive for CD31 and active caspase-3 in the GCL, hilus, and ML. Active caspase-3-positive cells were further magnified and examined in their full *z*-dimension. The analysis was performed on every 12th section, with an average of four to five analyzed sections per hippocampus.

Analysis of the Neurovascular Niche

A confocal Leica TCS SP2 microscope was used to measure the distance between BLBP-positive neural stem cells and CD31-positive microvessels. Confocal images were acquired of a minimum of 40 cells per subgranular

zone and sections for analysis were picked randomly. The distance was measured in the *x*–*y* plane from the edge of the BLBP-labeled cell to the edge of the nearest vessel using Adobe Illustrator CS6 (San Jose, CA, USA).

Statistical Analysis

All data are presented as mean ± s.e.m. The data were compared using independent samples *t*-test (SPSS, PASW Statistics 17.0, IBM, New York, NY, USA) and significance levels were set to: $^{*}P<0.05$, $^{**}P<0.01$, and $^{***}P<0.001$.

RESULTS

Irradiation Altered Microvessel Structure and Complexity in Both Neurogenic and Nonneurogenic Hippocampal Areas

The main focus of this study was to investigate how microvessels in both neurogenic (i.e., the GCL) and nonneurogenic (i.e., the hilus and the ML) hippocampal areas respond to whole-brain irradiation. At the age of P14, mice were irradiated with a single dose of 8 Gy. Microvessels were then histologically visualized through a staining with cluster of differentiation 31 (CD31, also called PECAM-1), which is present in the intercellular junctions of both human and murine endothelial cells where it contributes to cell adhesion.[20,21]

First, the total area covered by microvessels was quantified (Figure 1A). A reduction in the total microvessel area was found in irradiated mice compared with control mice in all investigated structures with an overall decrease of 25–30% 1 week after irradiation. In the GCL, a decrease was observed 1 week (0.92 ± 0.05 versus $0.70\pm0.04\,mm^2$; $P<0.01$) and 7 weeks after irradiation (0.92 ± 0.04 versus $0.70\pm0.04\,mm^2$; $P<0.01$) (Figure 1B). Similarly, the hilus was reduced 1 week after irradiation (0.68 ± 0.05 versus $0.48\pm0.04\,mm^2$; $P<0.01$) (Figure 1C) and the ML was reduced both 1 week (2.43 ± 0.23 versus $1.70\pm0.08\,mm^2$; $P<0.01$) and 7 weeks after irradiation (2.77 ± 0.16 versus $2.15\pm0.14\,mm^2$; $P<0.05$) (Figure 1D). No difference was observed in the hilus of the 7-week group, or in any of the investigated structures of the 1-year group (Figures 1B–1D). The irradiation-induced decrease in total microvessel area was hence most pronounced after 1 week, less pronounced after 7 weeks, and not detectable after 1 year.

Second, we found that irradiation led to a decrease in the total number of microvessels (Figure 2A). This was seen in both the neurogenic (Figure 2B) and the nonneurogenic areas (Figures 2C and 2D). The reduction in the GCL persisted from 1 week ($9,218\pm362$ versus $6,920\pm263$; $P<0.001$), through 7 weeks ($8,380\pm465$ versus $6,159\pm386$; $P<0.01$) up to 1 year after irradiation ($7,479\pm379$ versus $6,127\pm182$; $P<0.01$). The hilus showed a decrease 1 week ($6,482\pm576$ versus $4,778\pm301$; $P<0.01$) and 7 weeks ($6,936\pm617$ versus $5,112\pm322$; $P<0.05$), but not 1 year after irradiation. As in the GCL, the ML was reduced at all three time points (1 week; $18,921\pm1,152$ versus $14,265\pm712$; $P<0.01$, 7 weeks; $21,763\pm1,310$ versus $17,499\pm892$; $P<0.05$, 1 year; ($18,301\pm669$ versus $15,761\pm606$; $P<0.05$).

Third, the diameter of the microvessels (capillaries) was measured and a smaller microvessel diameter was observed in the hilus of irradiated mice compared with control mice 1 week after irradiation (4.80 ± 0.06 in controls versus $4.28\pm0.13\,\mu m$ in irradiated mice; $P<0.01$). No other differences were detected at any other time points or in any other structures (data not shown) and we therefore draw the conclusion that microvessel diameter was relatively unaffected by irradiation.

To evaluate whether irradiation affected microvessel complexity,[22] we quantified the total number of branching points (Figure 3A). Irradiated mice had a reduced number of branching points compared with control mice at all three time points in the GCL (1 week; 617 ± 42 versus 502 ± 17; $P<0.05$, 7 weeks; 628 ± 68 versus $368\pm\pm32$; $P<0.01$, 1 year; 468 ± 40 versus 346 ± 28; $P<0.05$) (Figure 3B). In the nonneurogenic areas, no difference was observed 1 week after irradiation, but after 7 weeks both the hilus (514 ± 37 versus 364 ± 34; $P<0.05$) (Figure 3C) and the ML ($2,702\pm245$ versus $2,124\pm83$; $P<0.05$) (Figure 3D) showed a reduced number of branching points in irradiated animals. Hence, the reduction of vessels was most pronounced in the neurogenic GCL.

Persistent Volume Changes in the Hippocampal Granule Cell Layer and Molecular Layer up to 1 year After Irradiation

Alterations in brain growth after irradiation to the developing brain have been demonstrated earlier[23–25] and might have negative effects on hippocampal structure and function. We therefore assessed if irradiation affected the total volumes of the GCL, hilus, or ML.

Acutely, 6 hours after irradiation, no differences were observed between irradiated and control mice in any subregion (left panel, Figures 4B–4D). A smaller GCL volume was found at all other

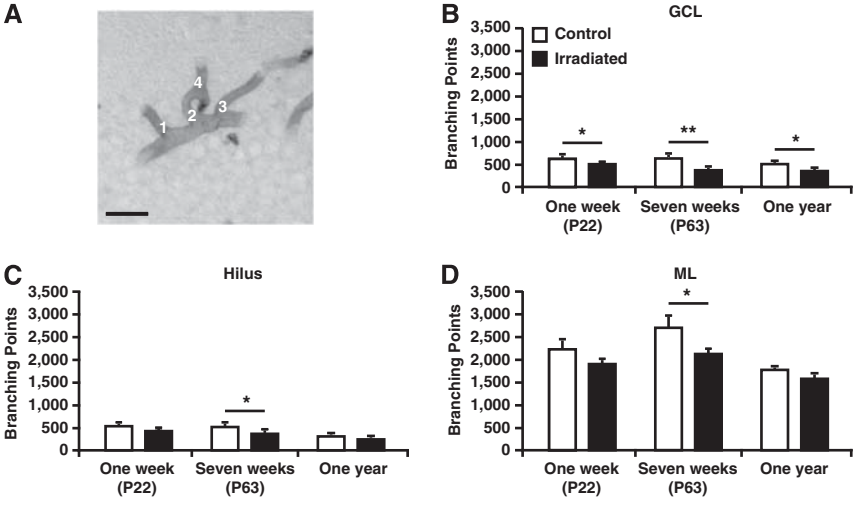

Figure 3. All branching points were counted in the granule cell layer (GCL), hilus, and molecular layer (ML) of the dentate gyrus. (**A**) Representative picture with numbers (1–4) where there is a microvessel branching point. The graphs show quantifications 1 week, 7 weeks, and 1 year after irradiation in the GCL (**B**), hilus (**C**), and ML (**D**). Postnatal day (P), $n=6$ per group, group mean values ± s.e.m., scale bar = 20 μm, $^{*}P<0.05$, $^{**}P<0.01$.

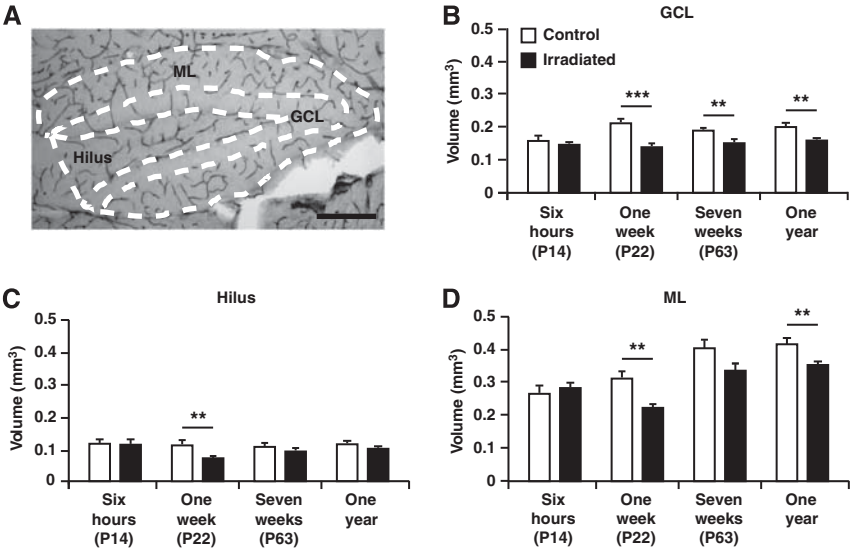

Figure 4. Volume of the granule cell layer (GCL), hilus, and molecular layer (ML) of the dentate gyrus. (**A**) Representative picture showing the CD31 microvessel staining in the dentate gyrus and schematic drawings of how the three regions were traced. The graphs show measurements 6 hours, 1 week, 7 weeks, and 1 year after irradiation in the GCL (**B**), hilus (**C**), and ML (**D**). Postnatal day (P), $n = 6$ per group, group mean values ± s.e.m., scale bar = 200 μm, $^{**}P < 0.01$, $^{***}P < 0.001$.

investigated time points (1 week; 0.21 ± 0.01 versus $0.14 \pm 0.006\,mm^3$; $P < 0.001$, 7 weeks; 0.19 ± 0.006 versus $0.15 \pm 0.006\,mm^3$; $P < 0.01$, 1 year; 0.20 ± 0.008 versus $0.16 \pm 0.004\,mm^3$; $P < 0.01$) (Figure 4B). The volume of the hilus, on the other hand, was only reduced 1 week after irradiation (0.11 ± 0.009 versus $0.07 \pm 0.003\,mm^3$; $P < 0.01$) (Figure 4C). The ML was reduced 1 week after irradiation (0.31 ± 0.018 versus $0.22 \pm 0.012\,mm^3$; $P < 0.01$) and the decrease appeared to persist up to 1 year after irradiation (0.41 ± 0.016 versus $0.35 \pm 0.009\,mm^3$; $P < 0.01$), however, not significant at 7 weeks after irradiation (Figure 4D). All investigated structures of irradiated mice hence displayed an initial arrested growth compared with control mice 1 week after irradiation. Importantly, as for most of the measured microvessel parameters, the reduction in irradiated compared with control mice diminished with time.

Microvessel Density Increased Early and Transiently in Irradiated Brains

As all quantifications of microvessel parameters and volume measurements followed the same trend, that is, the reduction in irradiated compared with control mice diminished with time, we also wanted to calculate the densities. To our surprise, we found that irradiated animals displayed a significantly higher density of branching points in the GCL 1 week after irradiation, followed by a reduced density of branching points in irradiated animals at 7 weeks after irradiation (Table 1A). Also in the hilus, irradiated animals displayed an increased density of branching points 1 week after irradiation, followed by a decreased density of microvessels 7 weeks after irradiation in irradiated animals (Table 1B). Similarly, irradiated animals in the ML displayed an increased density of branching points at 1 week after irradiation (Table 1C). At 1 year after irradiation, no differences were observed between control and irradiated mice for any of the microvessel density parameters.

Neurogenesis Was Decreased both Short-Term and Long-Term After Irradiation

After analyzing the structure and complexity of the vasculature, we sought to verify the detrimental effects of irradiation on neurogenesis, as shown in earlier studies.[25,26] Sections were stained for DCX to identify immature neuronal precursor cells and the total number of DCX-positive cells in the GCL including the subgranular zone (SGZ) was quantified. Irradiation drastically decreased the number of DCX-positive cells 1 week ($28{,}297 \pm 1{,}201$ versus $6{,}520 \pm 1{,}054$; $P < 0.001$), 7 weeks ($10{,}702 \pm 760$ versus $2{,}296 \pm 773$; $P < 0.001$), and 1 year (530 ± 66 versus 10 ± 4; $P < 0.001$) after irradiation (Figure 5). The numbers of DCX-positive cells in irradiated mice compared with age-matched control mice were 77% fewer at 1 week, 86% fewer at 7 weeks, and 98% fewer at 1 year after irradiation. Hence, the irradiation-induced decrease in neurogenesis showed no signs of recovery over time, rather the opposite. In addition, in nonirradiated control brains, the numbers of DCX-positive cells declined with age from 1 week to 1 year. The numbers of DCX-positive cells were 66% fewer at 7 weeks and 98% fewer at 1 year, compared with the 1 week time point (3 weeks of age).

Irradiation to the Young Brain Did Not Alter the Neurovascular Niche

To address what role microvessels may have in the support and maintenance of hippocampal neurogenesis and if this neurovascular niche is affected by irradiation to the young brain, we measured the distance between undifferentiated neural stem cells and the nearest microvessel.[16] The distance to the nearest microvessel (CD31-positive structure) from at least 40 stem cells (BLBP-positive) per SGZ was measured 7 weeks after irradiation (Figure 6A). The average distance was not different between controls and irradiated brains (8.47 ± 0.59 versus 9.96 ± 0.44 μm; $P = 0.073$). When analyzing the distance in more detail, the tendency to an increased distance in irradiated hippocampi was attributable to the cells located >15 μm from a microvessel, that is, a longer distance where direct contact is unlikely and diffusion would be less efficient. For the stem cells more closely located to microvessels, there was no tendency to a greater distance in irradiated brains (Figure 6B). We also stained for dying endothelial cells 6 hours after irradiation. In nonirradiated hippocampi, no dying endothelial cells (double positive for active caspase-3 and CD31) were detected (Figure 6C, left panel). Large numbers of dying cells positive for active caspase-3 were visible in the SGZ of irradiated animals (Figure 6C, right panel), but virtually

Table 1. Densities (number/mm^3) for the vessel number and number of branching points presented in the GCL (A), hilus (B), and ML (C) 1 week, 7 weeks, and 1 year after irradiation

(A) GCL						
Density (number/mm^3)	*One week (P22)*		*Seven weeks (P63)*		*One year*	
	C	*Irr*	*C*	*Irr*	*C*	*Irr*
Vessel number	43,529 (± 2,916)	49,827 (± 2,602)	44,234 (± 2,000)	40,766 (± 1,367)	37,633 (± 1,944)	38,271 (± 1,241)
Branching points	2,912 (± 181)	3,612* (± 179)	3,314 (± 288)	2,435* (± 225)	2,355 (± 243)	2,162 (± 203)
(B) Hilus						
Density (number/mm^3)	*One week (P22)*		*Seven weeks (P63)*		*One year*	
	C	*Irr*	*C*	*Irr*	*C*	*Irr*
Vessel number	57,387 (± 3,914)	65,841 (± 1,170)	61,999 (± 1,850)	52,778* (± 2,557)	43,833 (± 3,301)	44,174 (± 1,941)
Branching points	4,871 (± 368)	6,058* (± 352)	4,916 (± 348)	4,021 (± 557)	2,609 (± 113)	2,495 (± 95)
(C) ML						
Density (number/mm^3)	*One week (P22)*		*Seven weeks (P63)*		*One year*	
	C	*Irr*	*C*	*Irr*	*C*	*Irr*
Vessel number	60,524 (± 4,451)	63,830 (± 1,535)	53,733 (± 1,294)	51,980 (± 1,551)	44,168 (± 1,266)	44,515 (± 1,475)
Branching points	7,117 (± 422)	8,502* (± 278)	6,671 (± 384)	6,309 (± 333)	4,204 (± 204)	4,463 (± 234)

Abbreviations: GCL, granule cell layer; ML, molecular layer. Postnatal day (P), $n = 6$ per group, group mean values ± s.e.m., $^*P < 0.05$.

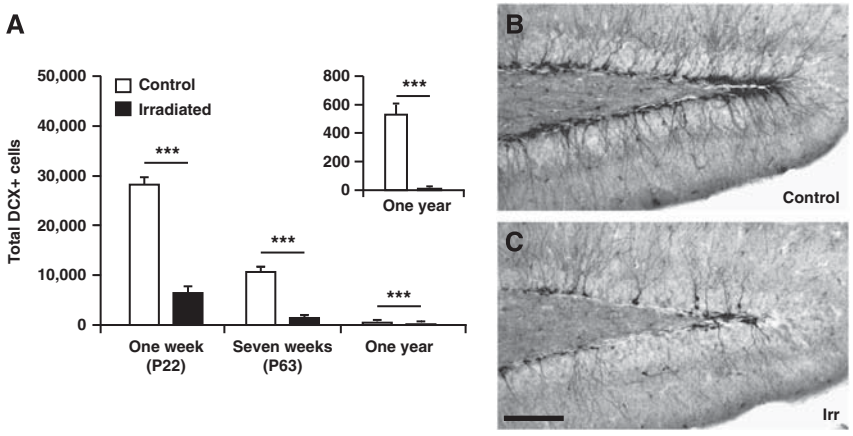

Figure 5. (**A**) The graph shows the results from quantification of DCX$^+$ cells 1 week, 7 weeks, and 1 year after irradiation. The relative loss of DCX-positive cells in irradiated mice compared with age-matched control mice increased with time (77% decreased at 1 week (P22), 86% decreased at 7 weeks (P63), and 98% decreased at 1 year after irradiation). Representative pictures depicting the DCX staining 7 weeks after irradiation in control (**B**) and irradiated (**C**) animals. Postnatal day (P), $n = 6$ per group, group mean values ± s.e.m., scale bar = 100 μm, $^{***}P < 0.001$. DCX, doublecortin.

none of them was also positive for CD31. Only 14.0 ± 4.1 dying endothelial cells, positive for both active caspase-3 and CD31, could be detected per hippocampus, and these cells were detected throughout the hippocampus, not just in the SGZ, where most cell death was occurring.

DISCUSSION

In the present study we demonstrated that a single radiation dose of 8 Gy to the young, still developing mouse brain reduced microvessel area, number of microvessels and the number of microvessel branching points in the hippocampus at three different time points after irradiation. Early (1 week) after irradiation, the absolute numbers of microvessels and branching points were decreased. However, the densities of microvessel branching points were increased at this time point, indicating that the surrounding neural and glial tissue initially was more affected than the vascular tissue. At the later time points, the densities were gradually normalized, demonstrating the microvasculature's capacity to adapt to the surrounding tissue. We also confirmed and extended previous studies reporting that irradiation reduces the pool of neural progenitor cells and leads to a persistently decreased level of neurogenesis.[16,23,25,27,28] In addition, we verify both the natural decline in hippocampal neurogenesis with age,[29] as well as clearly demonstrate the detrimental effect of irradiation on immature neurons, such that neurogenesis deteriorated more

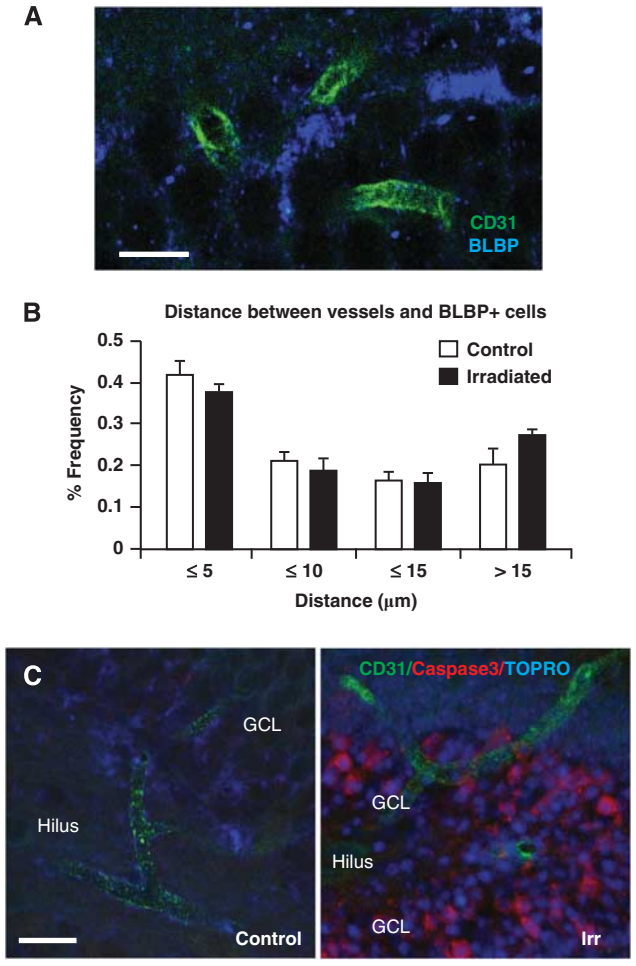

Figure 6. Irradiation to the young brain did not disrupt the vascular niche or cause acute endothelial cell death. (**A**) Representative image of the staining used to measure the distance between undifferentiated neural stem cells; brain lipid-binding protein (BLBP)-positive (blue), and microvessels; CD31-positive (green) 7 weeks after irradiation (P63). (**B**) The graph shows the frequency of BLBP-positive cells located at different distance intervals to the nearest microvessel. There were no differences in the distribution between irradiated and control animals, and the majority of the cells lie in close proximity to a microvessel ($\leqslant 5\,\mu$m). (**C**) Representative pictures of the staining used to investigate endothelial cell death 6 hours after irradiation; active caspase-3 (red), CD31 (green) and nuclear stain, TO-PRO-3 (blue). A control animal in the left panel and an irradiated animal in the right panel. $N = 6$ per group, group mean values ± s.e.m., scale bar = 10 μm (**A**) and 20 μm (**B**).

rapidly after irradiation and showed no signs of recovery up to 1 year after irradiation.

Irradiation Caused Growth Arrest During Normal Development of the Brain

Our results show significant volume differences in the GCL and ML up to 1 year after irradiation. A general brain volume loss in children,[9] as well as specifically smaller hippocampal volumes in both rats[24] and mice[25,30] have previously been reported following irradiation. In humans, as well as in rodents, the brain, and particularly the hippocampus, continues to grow postnatally and shows an exponential growth in early childhood until a plateau phase and maximal brain volume is reached at adolescence.[31,32] Hence, irradiation in this model of juvenile mice targets the brain in a phase when it is still continuously developing and growing. The smaller volume observed after irradiation is therefore most likely explained by arrested growth, resulting in reduced volumes in irradiated brains compared with control brains.[26] Cell death may also contribute to the smaller volumes through an acute loss of cells,[24,30] and the corresponding volume. This is most evident in areas where postnatal neurogenesis occurs. Here, we demonstrate that also neighboring, nonneurogenic regions (the hilus and the ML), where no overt cell death occurs, display growth retardation. Irradiation has previously been demonstrated to cause a more profound effect on hippocampal volume in the young (immature) brain, as compared with irradiation to the brains of older animals.[23] In addition, the relative differences between irradiated and control brains in the current study decreased with time, indicating a partial volume recovery (Figure 4).

The Vasculature Adjusted to the Surrounding Neural Tissue

When calculating the densities for the blood vessel parameters, we found that irradiated animals had a significantly higher density of branching points in all three regions investigated 1 week after irradiation. This suggests that even though the total volume of the vascular bed was reduced, the surrounding tissue displayed an even more pronounced volume loss and growth arrest. However, 7 weeks after irradiation, all densities except branching points in the GCL and microvessels in the hilus, were normalized compared with controls, indicating that the vasculature had in fact adjusted to the new environmental conditions at this time point. This was confirmed by the latest time point, 1 year after irradiation, when all vascular densities were normalized. Taken together, this indicates that the surrounding tissue regulates the dynamics of the vasculature. In contrast, Warrington *et al*[17] subjected adult mice to 8×4.5 Gy cranial irradiation over a period of 4 weeks and 1 month later they found decreased capillary densities in the dentate gyrus. The radiation dose in that study was however considerably higher than the dose used in our study, the brains were adult and consequently no longer growing. Supporting our findings, Ljubimova *et al*[18] subjected adult rats to 25 Gy whole-brain irradiation and found no difference in vessel density. In addition, Panagiotakos *et al*[19] subjected adult rats to 25 Gy cranial irradiation and found significant decreases of capillary segments and capillary length in the cortex and corpus callosum 1 day after irradiation but swift and persistent recovery of the vasculature up to 15 months after irradiation. Our findings indicate that the surrounding neural and glial tissue regulates the dynamics of the vasculature rather than the other way around. This is still an open question in the field, inspired by the seminal publication of Palmer *et al*,[14] demonstrating that dividing cells in the adult rat SGZ were found in dense clusters associated with the vasculature and that roughly 37% of all dividing cells were immunoreactive for endothelial markers, suggesting that neurogenesis is intimately associated with a process of active vascular recruitment and subsequent remodeling. Our study differed from theirs in that we quantified all microvessels in the dentate gyrus, not only the ones closely associated with proliferating progenitors.

Irradiation and the Neurovascular Niche

Neurogenesis has previously been shown to be persistently reduced in the hippocampus after irradiation.[13,23,26–28] We found a robust decrease in the number of neuronally committed progenitors in the hippocampal GCL at all three time points investigated. Furthermore, the difference between irradiated and control mice increased with time. Monje *et al*[16] have shown that irradiated precursor cells still possess the capacity to differentiate into neurons *in vitro*. However, grafting of nonirradiated neural stem/precursor cells into the hippocampus of irradiated animals generated 81% fewer neurons *in vivo* compared with grafted cells in control rats. The survival of the grafted cells was comparable between irradiated and control animals, but there

was a corresponding increase in the number of cells adopting a glial (NG2) fate. Hence, not only was hippocampal neurogenesis ablated through acute progenitor cell death, but the remaining neural precursors adopted glial fates to a higher extent than normal. This implies that the decrease in neurogenesis after irradiation is not caused by an intrinsic defect of the progenitor cells, but could rather be an effect of a chronic inflammation in the surrounding microenvironment. However, adult and immature rat brains display different inflammatory responses to irradiation. For example, adult brains displayed increased levels of interleukin-6 and chronic inflammation after irradiation,[16,33] whereas the immature rat brain displayed decreased levels of interleukin-6 and only transient inflammation.[34] Divergent opinions exist concerning the relationship between stem cell niches and the microvasculature after irradiation. It has been proposed that irradiation disrupts the normal hippocampal neurovascular niche where newborn cells cluster on and around the vasculature in control animals. For instance, Monje *et al*[16] have also shown that the distance between a BrdU-positive neural precursor cell and the nearest located microvessel increased in irradiated compared with control mice. The BrdU-labeled cells in the study by Monje *et al* constitute a heterogeneous population of cells, being labeled once daily for 6 days and analyzed on the 7th day. In the current study, we have measured the distance between undifferentiated neural stem cells (BLBP-positive, so called type I cells) and the nearest microvessel. The distance was not altered by irradiation, arguing against a role for microvessel injury being an upstream event in the loss of neural stem/progenitor cells or the perturbation of neurogenesis, at least in the young mouse brain. In addition, others have emphasized the importance of microvessels in radiotherapy since preventing endothelial apoptosis pharmacologically could rescue stem cell dysfunction of the intestinal crypt.[35] Furthermore, the vascular-specific radioprotective agent WR-2721 (amifostine, Ethyol), which does not pass the blood–brain barrier, could decrease the number of animals developing radionecrosis following 25 Gy irradiation to the brain.[36] On the other hand, the importance and involvement of microvessels in stem cell ablation after irradiation has been questioned in a study by Otsuka *et al*.[37] They compared the effect on immature neural precursor cells when targeting the vessels specifically or the parenchyma uniformly and found that the neural precursor cells where less affected when the irradiation targeted only the microvasculature compared with the entire parenchyma, indicating that other factors than microvessels contribute to the irradiation-induced damage. Our study revealed only a handful of dying endothelial cells in the entire irradiated hippocampus, in stark contrast to the tens of thousands of dying stem and progenitor cells in the SGZ.[30] This strongly speaks against a role for injury to microvessels being a primary event in the perturbation of neurogenesis in the hippocampus. We speculate that the developmental stage of the brains and the irradiation dose used can explain many of the differences observed.

Implications of the Study

Survivors of childhood leukemia and brain tumors, particularly those with brain tumors treated with radiation therapy at doses of $\geq$30 Gy, are at an increased risk of stroke due to subsequent vasculopathies with the risk of stroke being dose-related.[38,39] Compared with unaffected siblings, the relative risk of stroke is almost 10 times higher in survivors of all childhood cancers,[40] but the underlying mechanisms are poorly understood. Our research group has previously demonstrated that the immature and still growing rat hippocampus is more susceptible to irradiation,[23] and it has been proposed that even very low doses of irradiation during infancy may produce cognitive deficits that persist into adulthood.[41] It is therefore important to investigate the acute and late effects of radiation to the brain. Specifically, understanding the roles that blood vessels play in intrinsic support and maintenance of stem cell populations may provide novel ways to improve the hippocampal microenvironment and could thereby provide a neurobiological basis for protective strategies after irradiation to the young brain. If we can mitigate the adverse side-effects of radiation therapy in the increasing number of survivors of childhood cancer, we could improve their quality of life.

DISCLOSURE/CONFLICT OF INTEREST

The authors declare no conflict of interest.

ACKNOWLEDGEMENTS

The authors are grateful to the skillful technical assistance of Rita Grandér. The authors thank Michelle Porritt for fruitful input. The funding agencies had no influence on the study design.

REFERENCES

1 Parkin DM, Stiller CA, Draper GJ, Bieber CA. The international incidence of childhood cancer. *Int J Cancer* 1988; **42**: 511–520.
2 Steliarova-Foucher E, Stiller C, Kaatsch P, Berrino F, Coebergh JW, Lacour B *et al.* Geographical patterns and time trends of cancer incidence and survival among children and adolescents in Europe since the 1970s (the ACCISproject): an epidemiological study. *Lancet* 2004; **364**: 2097–2105.
3 Schmidt LS, Schmiegelow K, Lahteenmaki P, Trager C, Stokland T, Grell K *et al.* Incidence of childhood central nervous system tumors in the Nordic countries. *Pediatr Blood Cancer* 2011; **56**: 65–69.
4 Mulhern RK, Khan RB, Kaplan S, Helton S, Christensen R, Bonner M *et al.* Short-term efficacy of methylphenidate: a randomized, double-blind, placebo-controlled trial among survivors of childhood cancer. *J Clin Oncol* 2004; **22**: 4795–4803.
5 Ellenberg L, Liu Q, Gioia G, Yasui Y, Packer RJ, Mertens A *et al.* Neurocognitive status in long-term survivors of childhood CNS malignancies: a report from the Childhood Cancer Survivor Study. *Neuropsychology* 2009; **23**: 705–717.
6 Haddy N, Mousannif A, Tukenova M, Guibout C, Grill J, Dhermain F *et al.* Relationship between the brain radiation dose for the treatment of childhood cancer and the risk of long-term cerebrovascular mortality. *Brain* 2011; **134**: 1362–1372.
7 Tam SJ, Watts RJ. Connecting vascular and nervous system development: angiogenesis and the blood-brain barrier. *Annu Rev Neurosci* 2010; **33**: 379–408.
8 Mukouyama YS, Shin D, Britsch S, Taniguchi M, Anderson DJ. Sensory nerves determine the pattern of arterial differentiation and blood vessel branching in the skin. *Cell* 2002; **109**: 693–705.
9 McDonald LW, Hayes TL. The role of capillaries in the pathogenesis of delayed radionecrosis of brain. *Am J Pathol* 1967; **50**: 745–764.
10 Wakisaka S, O'Neill RR, Kemper TL, Verrelli DM, Caveness WF. Delayed brain damage in adult monkeys from radiation in the therapeutic range. *Radiat Res* 1979; **80**: 277–291.
11 O'Connor MM, Mayberg MR. Effects of radiation on cerebral vasculature: a review. *Neurosurgery* 2000; **46**: 138–149, discussion 150-131.
12 Kuhn HG, Blomgren K. Developmental dysregulation of adult neurogenesis. *Eur J Neurosci* 2011; **33**: 1115–1122.
13 Raber J, Rola R, LeFevour A, Morhardt D, Curley J, Mizumatsu S *et al.* Radiation-induced cognitive impairments are associated with changes in indicators of hippocampal neurogenesis. *Radiat Res* 2004; **162**: 39–47.
14 Palmer TD, Willhoite AR, Gage FH. Vascular niche for adult hippocampal neurogenesis. *J Comp Neurol* 2000; **425**: 479–494.
15 Louissaint Jr. A, Rao S, Leventhal C, Goldman SA. Coordinated interaction of neurogenesis and angiogenesis in the adult songbird brain. *Neuron* 2002; **34**: 945–960.
16 Monje ML, Mizumatsu S, Fike JR, Palmer TD. Irradiation induces neural precursor-cell dysfunction. *Nat Med* 2002; **8**: 955–962.
17 Warrington JP, Csiszar A, Johnson DA, Herman TS, Ahmad S, Lee YW *et al.* Cerebral microvascular rarefaction induced by whole brain radiation is reversible by systemic hypoxia in mice. *Am J Physiol Heart Circ Physiol* 2011; **300**: H736–H744.
18 Ljubimova NV, Levitman MK, Plotnikova ED, Eidus L. Endothelial cell population dynamics in rat brain after local irradiation. *Br J Radiol* 1991; **64**: 934–940.
19 Panagiotakos G, Alshamy G, Chan B, Abrams R, Greenberg E, Saxena A *et al.* Long-term impact of radiation on the stem cell and oligodendrocyte precursors in the brain. *PLoS One* 2007; **2**: e588.

20 Albelda SM, Muller WA, Buck CA, Newman PJ. Molecular and cellular properties of PECAM-1 (endoCAM/CD31): a novel vascular cell-cell adhesion molecule. *J Cell Biol* 1991; **114**: 1059–1068.
21 Newman PJ, Berndt MC, Gorski J, White 2nd GC, Lyman S, Paddock C *et al.* PECAM-1 (CD31) cloning and relation to adhesion molecules of the immunoglobulin gene superfamily. *Science* 1990; **247**: 1219–1222.
22 Zhang L, Cooper-Kuhn CM, Nannmark U, Blomgren K, Kuhn HG. Stimulatory effects of thyroid hormone on brain angiogenesis in vivo and in vitro. *J Cereb Blood Flow Metab* 2010; **30**: 323–335.
23 Fukuda A, Fukuda H, Swanpalmer J, Hertzman S, Lannering B, Marky I *et al.* Age-dependent sensitivity of the developing brain to irradiation is correlated with the number and vulnerability of progenitor cells. *J Neurochem* 2005; **92**: 569–584.
24 Fukuda H, Fukuda A, Zhu C, Korhonen L, Swanpalmer J, Hertzman S *et al.* Irradiation-induced progenitor cell death in the developing brain is resistant to erythropoietin treatment and caspase inhibition. *Cell Death Differ* 2004; **11**: 1166–1178.
25 Naylor AS, Bull C, Nilsson MK, Zhu C, Bjork-Eriksson T, Eriksson PS *et al.* Voluntary running rescues adult hippocampal neurogenesis after irradiation of the young mouse brain. *Proc Natl Acad Sci USA* 2008; **105**: 14632–14637.
26 Roughton K, Kalm M, Blomgren K. Sex-dependent differences in behavior and hippocampal neurogenesis after irradiation to the young mouse brain. *Eur J Neurosci* 2012; **36**: 2763–2772.
27 Hellstrom NA, Bjork-Eriksson T, Blomgren K, Kuhn HG. Differential recovery of neural stem cells in the subventricular zone and dentate gyrus after ionizing radiation. *Stem Cells* 2009; **27**: 634–641.
28 Kalm M, Karlsson N, Nilsson MKL, Blomgren K. Loss of hippocampal neurogenesis, increased motor activity and impaired reversal learning one year after irradiation of the young mouse brain. *Exp Neurol* 2013; doi:10.1016/j.expneurol.2013.1001.1006 (in press).
29 Kuhn HG, Dickinson-Anson H, Gage FH. Neurogenesis in the dentate gyrus of the adult rat: age-related decrease of neuronal progenitor proliferation. *J Neurosci* 1996; **16**: 2027–2033.
30 Huo K, Sun Y, Li H, Du X, Wang X, Karlsson N *et al.* Lithium reduced neural progenitor apoptosis in the hippocampus and ameliorated functional deficits after irradiation to the immature mouse brain. *Mol Cell Neurosci* 2012; **51**: 32–42.
31 Courchesne E, Chisum HJ, Townsend J, Cowles A, Covington J, Egaas B *et al.* Normal brain development and aging: quantitative analysis at in vivo MR imaging in healthy volunteers. *Radiology* 2000; **216**: 672–682.
32 Zhang J, Miller MI, Plachez C, Richards LJ, Yarowsky P, van Zijl P *et al.* Mapping postnatal mouse brain development with diffusion tensor microimaging. *Neuroimage* 2005; **26**: 1042–1051.
33 Monje ML, Toda H, Palmer TD. Inflammatory blockade restores adult hippocampal neurogenesis. *Science* 2003; **302**: 1760–1765.
34 Kalm M, Fukuda A, Fukuda H, Ohrfelt A, Lannering B, Bjork-Eriksson T *et al.* Transient inflammation in neurogenic regions after irradiation of the developing brain. *Radiat Res* 2009; **171**: 66–76.
35 Paris F, Fuks Z, Kang A, Capodieci P, Juan G, Ehleiter D *et al.* Endothelial apoptosis as the primary lesion initiating intestinal radiation damage in mice. *Science* 2001; **293**: 293–297.
36 Lyubimova N, Hopewell JW. Experimental evidence to support the hypothesis that damage to vascular endothelium plays the primary role in the development of late radiation-induced CNS injury. *Br J Radiol* 2004; **77**: 488–492.
37 Otsuka S, Coderre JA, Micca PL, Morris GM, Hopewell JW, Rola R *et al.* Depletion of neural precursor cells after local brain irradiation is due to radiation dose to the parenchyma, not the vasculature. *Radiat Res* 2006; **165**: 582–591.
38 Bowers DC, Liu Y, Leisenring W, McNeil E, Stovall M, Gurney JG *et al.* Late-occurring stroke among long-term survivors of childhood leukemia and brain tumors: a report from the Childhood Cancer Survivor Study. *J Clin Oncol* 2006; **24**: 5277–5282.
39 Zhu C, Huang Z, Gao J, Zhang Y, Wang X, Karlsson N *et al.* Irradiation to the immature brain attenuates neurogenesis and exacerbates subsequent hypoxic-ischemic brain injury in the adult. *J Neurochem* 2009; **111**: 1447–1456.
40 Oeffinger KC, Mertens AC, Sklar CA, Kawashima T, Hudson MM, Meadows AT *et al.* Chronic health conditions in adult survivors of childhood cancer. *N Engl J Med* 2006; **355**: 1572–1582.
41 Hall P, Adami HO, Trichopoulos D, Pedersen NL, Lagiou P, Ekbom A *et al.* Effect of low doses of ionising radiation in infancy on cognitive function in adulthood: Swedish population based cohort study. *BMJ* 2004; **328**: 19.